FOURTH EUROPEAN ROTORCRAFT AND POWERED LIFT AIRCRAFT FORUM

Paper No. 25

THE INFLUENCE OF HIGH TWIST ON THE DYNAMICS OF ROTATING BLADES

William F. White, Jr.

Structures Laboratory
US Army Research and Technology Laboratories
(AVRADCOM)
Langley Research Center
Hampton, Virginia, USA

September 13 - 15, 1978

STRESA - ITALY

Associazione Italiana di Aeronautica ed Astronautica

Associazione Industrie Aerospaziali

THE INFLUENCE OF HIGH TWIST ON THE DYNAMICS OF ROTATING BLADES

William F. White, Jr.

Structures Laboratory
US Army Research and Technology Laboratories
(AVRADCOM)
Langley Research Center
Hampton, Virginia, USA

1. SUMMARY

A method is presented for determining the free vibration characteristics of a rotating blade having high twist and nonuniform spanwise properties. The equations which govern the bending and torsional motion of such a blade are solved using a generalized integration matrix as the basis of the method of solution. By using this matrix as an operator on the equations expressed in matrix notation, the differential equations are numerically integrated to eliminate the spatial dependence and reduced to familiar matrix eigenvalue form from which the dynamics of the blade are determined using standard eigenvalue extraction techniques. The application of this technique to problems of this type offers several computational advantages over other methods of solution. Numerical results using the present method of solution are in good agreement with experimental results.

2. SYMBOLS

B_1, B_2	Blade section constants
E	Young's modulus of elasticity
G	Shear modulus of elasticity
I_1, I_2	Cross-section area moments of inertia
J	Torsional stiffness constant
k_a	Polar radius of gyration of cross-sectional area effective in carrying tension

k_m	Polar radius of gyration of cross-sectional mass about elastic axis ($k_m^2 = k_{m_1}^2 + k_{m_2}^2$)
k_{m_1}, k_{m_2}	Mass radii of gyration about major neutral axis and about an axis perpendicular to chord through the elastic axis, respectively
m	Mass per unit length
n	Number of blade stations
R	Blade radius
T	Blade tension, $T \cong \int_x^R \Omega^2 mx\, dx$
v,w	Lateral displacements of beam, in plane of rotation and normal to plane, respectively
$\bar{v},\bar{w}$	Vibration amplitude of v and w, respectively
x,y,z	Coordinate system which rotates with blade such that x-axis falls along initial or undeformed position of elastic axis
η	Variable of integration
θ	Blade angle prior to any deformation, positive when leading edge is up
Φ	Total torsional deflection, $\Phi = \phi_o + \phi$, or eigenvector
ϕ	Elastic torsional deflection, positive when leading edge is up
ϕ_o	Steady-state twist
$\bar{\phi}$	Vibration amplitude of ϕ
Ω	Rotor angular velocity
ω	Natural frequency of vibration

Primes denote derivatives with respect to x; dots denote derivatives with respect to time

Matrix notation:

[ ]	Square matrix
⌈ ⌋	Diagonal matrix

{ }	Column matrix
$[\ ]^{-1}$	Inverted matrix
[1]	Unit or identity matrix

3. INTRODUCTION

The dynamic behavior of flexible rotating blades has received considerable attention in the literature for many years, both because it constitutes a fundamental problem in applied mechanics and because of the use of blades as parts of many rotating structures of engineering importance. Helicopters, propellers, and turbines may have serious resonant vibration problems when the excitation frequencies are equal to some multiple of the rotational speed. To insure that conditions susceptible to resonance do not exist within the range of operating speeds, it is necessary that the natural frequencies be determined accurately. Also, the natural modes, because of their orthogonality relationships, are often used in forced response and stability calculations.

This paper formulates a numerical solution of the natural vibration frequencies and mode shapes of a rotating blade having high twist and nonuniform spanwise properties. This problem has been treated analytically in a very complete development by Houbolt and Brooks.[1] However, very few results are presented, and they are for special cases of limited interest. The present analysis employs the governing equations derived in Reference 2 with the assumption of coincident elastic, mass and tension axes. The blade is allowed to have an arbitrary high pitch angle, which results in a nonlinear torsional elastic restoring moment. The governing equations are solved numerically using a generalized integration matrix as an operator on the equations expressed in matrix notation. The equations are linearized and reduced to familiar matrix eigenvalue form from which the dynamics of the blade are determined using standard eigenvalue extraction techniques. Numerical results using the present method of solution are in good agreement with experimental results.

4. FORMULATION

The equations of motion which describe the bending and torsional free vibrations of the blade shown in Figure (1) are derived in Reference 2. The local orientation of the major principal axis relative to the plane of rotation is composed of the geometric angles of pitch and pretwist. In the present analysis, the angular displacement about this undeformed position is the sum of the torsional elastic deformation and the steady-state twist. The steady-state twist may be a large angle and is dependent on blade characteristics (including pitch and pretwist) and rotational speed. This large steady-state angular displacement results in a nonlinear torsional internal elastic restoring moment. Specializing the equations of motion derived in Reference 2 for the case of torsional motion completely uncoupled from bending, the equations of interest assume the form

flapwise bending:

$$(EI_1 \cos^2\theta + EI_2 \sin^2\theta)w''(x,t) + (EI_2 - EI_1)\cos\theta \sin\theta\, v''(x,t) + \Omega^2 \int_x^R m\eta[w(\eta,t) - w(x,t)]d\eta = -\int_x^R m\ddot{w}(\eta,t)(\eta - x)d\eta \tag{1}$$

inplane bending:

$$(EI_2 - EI_1)\cos\theta \sin\theta\, w''(x,t) + (EI_1 \sin^2\theta + EI_2 \cos^2\theta)v''(x,t) + \Omega^2 \int_x^R m[xv(\eta,t) - \eta v(x,t)]d\eta = -\int_x^R m\ddot{v}(\eta,t)(\eta - x)d\eta \tag{2}$$

torsion:

$$\{GJ + EB_1[(\theta')^2 + \tfrac{3}{2}\theta'\Phi' + \tfrac{1}{2}(\Phi')^2]\}\Phi' + Tk_a^2(\theta' + \Phi') + \frac{\Omega^2}{2}\int_x^R m(k_{m_2}{}^2 - k_{m_1}{}^2)\sin 2(\theta + \Phi)\,d\eta = -\int_x^R mk_m^2\,\ddot{\Phi}\,d\eta \tag{3}$$

where Φ is the sum of the steady-state twist, ϕ_o, and the torsional elastic deformation ϕ

$$\Phi(x,t) = \phi_o(x) + \phi(x,t) \tag{4}$$

For the present analysis, fixed-free boundary conditions are assumed. Thus, displacements and slopes are zero at the root and shears and moments are zero at the tip.

Equation (3) is linearized about the steady-state angular position, ϕ_o, by assuming that ϕ is a perturbation quantity. Substituting equation (4) into equation (3) and setting all perturbation quantities equal to zero yields an equilibrium equation for ϕ_o

$$\{GJ + EB_1[(\theta')^2 + \tfrac{3}{2}\theta'\phi_o' + \tfrac{1}{2}(\phi_o')^2]\}\phi_o' + Tk_a^2(\theta' + \phi_o') + \frac{\Omega^2}{2}\int_x^R m(k_{m_2}{}^2 - k_{m_1}{}^2)\sin 2(\theta + \phi_o)d\eta = 0 \tag{5}$$

Substituting equation (4) into equation (3), substracting the equilibrium equation and discarding higher order products of perturbation quantities, yields the perturbation equation.

$$\{GJ + Tk_a^2 + EB_1[(\theta')^2 + \underline{\underline{3\theta'\phi_o'}} + \underline{\underline{\tfrac{3}{2}(\phi_o')^2}}]\}\phi' + \Omega^2\int_x^R m(k_{m_2}^2 - k_{m_1}^2)\phi\cos 2(\theta + \underline{\underline{\phi_o}})d\eta + \int_x^R m\,k_m^2\,\ddot{\phi}\,d\eta = 0 \tag{6}$$

The underlined terms in equation (6) are due to the nonlinear terms in equation (3). The steady-state twist ϕ_o is determined by iteration from equation (5). This value is used to determine the coefficients of equation (6) which is solved for the torsional frequencies.

Equations (1), (2), and (6) are linear equations, but have no closed form solution, and recourse must be made either to approximate methods of solution or direct numerical integration. Here, these equations are solved numerically by introducing a generalized integration matrix operator. By expressing these equations in matrix notation to isolate the fundamental derivatives[3] w'', v'', and ϕ', using the generalized integration matrix, and applying the boundary conditions, the equations reduce to a linear eigenvalue problem.

Equations (1), (2), and (6) are written at discrete points along the blade and the resulting sets of equations cast into matrix form. The integrals appearing in these matrix equations can be conveniently evaluated by introducing a generalized integration operator. This operator matrix is a means of numerically integrating a function that is expressed in terms of values of the function at increments of the independent variable. The generalized integration operator is defined as

$$\left\{\int_{x_o}^{x_i} f(x)dx\right\} = [I_1]\{f\} \qquad i = 0,1,2,\ldots,n \tag{7}$$

where $f(x)$ is an arbitrary function of x and $\{f\}$ is a column matrix which defines $f(x)$ at a discrete number of points or stations. The matrix $[I_1]$ may be viewed as a matrix operator where the premultiplication of a column matrix defining the function $f(x)$ by $[I_1]$ yields the numerical integration of $f(x)$ from x_o to x_i where $i = 0, 1, 2, \ldots, n$.

Inspection of equations (1), (2), and (6) indicates integrals that differ from type considered in equation (7). However, these additional types of integrals may be evaluated as a function of the matrix operator $[I_1]$. Using the generalized integration matrix as an operator in this manner, the solution of the differential equations can be developed entirely in matrix notation. However, to isolate the column of values of the fundamental derivatives as the dependent variables in the matrix equations, the relationships

$$
\begin{aligned}
v'(x,t) &= v'(o,t) + \int_o^x v''(x,t)dx \\
v(x,t) &= v(o,t) + \int_o^x v'(x,t)dx \\
w'(x,t) &= w'(o,t) + \int_o^x w''(x,t)dx \\
w(x,t) &= w(o,t) + \int_o^x w'(x,t) \\
\phi(x,t) &= \phi(o,t) + \int_o^x \phi'(x,t)dx
\end{aligned} \tag{8}
$$

are needed. Writing equation (8) at discrete points along the blade applying equation (7), and imposing the boundary conditions yields

$$
\begin{aligned}
\{v'\} &= [I_1]\ \{v''\} \\
\{v\} &= [I_1]\ \{v'\} = [I_1]\ [I_1]\ \{v''\} \\
\{w'\} &= [I_1]\ \{w''\} \\
\{w\} &= [I_1]\ \{w'\} = [I_1]\ [I_1]\ \{w''\} \\
\{\phi\} &= [I_1]\ \{\phi'\}
\end{aligned} \tag{9}
$$

Thus, all lower derivatives of the dependent variables (including the dependent variables themselves) which appear in the equations may be expressed as integrals of the fundamental derivatives w'', v'', and ϕ'. Using equations (7) and (9) equations (1), (2), and (6) may be expressed as a single matrix equation with respect to a column matrix having the fundamental derivatives for its elements. Assuming solutions of the form

$$
\begin{aligned}
\{v(x,t)\} &= \{\bar{v}(x)\}e^{i\omega t} \\
\{w(x,t)\} &= \{\bar{w}(x)\}e^{i\omega t} \\
\{\phi(x,t)\} &= \{\bar{\phi}(x)\}e^{i\omega t}
\end{aligned}
$$

and expressing the resulting equations of motion in matrix form yields

$$\begin{bmatrix} [G_{11}] & [G_{12}] & [0] \\ [G_{21}] & [G_{22}] & [0] \\ [0] & [0] & [G_{33}] \end{bmatrix} \begin{Bmatrix} \{\bar{w}''\} \\ \{\bar{v}''\} \\ \{\bar{\phi}'\} \end{Bmatrix} = \omega^2 \begin{bmatrix} [H_{11}] & [0] & [0] \\ [0] & [H_{22}] & [0] \\ [0] & [0] & [H_{33}] \end{bmatrix} \begin{Bmatrix} \{\bar{w}''\} \\ \{\bar{v}''\} \\ \{\bar{\phi}'\} \end{Bmatrix} \qquad (10)$$

where

$$[G_{11}] = \lceil EI_1 \cos^2 \theta + EI_2 \sin^2 \theta \rfloor + \Omega^2 \, [I_2(mx)][I_1][I_1]$$

$$[G_{12}] = [G_{21}] = \lceil (EI_2 - EI_1) \cos \theta \sin \theta \rfloor$$

$$[G_{22}] = \lceil EI_1 \sin^2 \theta + EI_2 \cos^2 \theta \rfloor - \Omega^2 \, [I_3]\lceil m \rfloor [I_1][I_1]$$

$$+ \Omega^2 \, [I_2(mx)][I_1][I_1]$$

$$[G_{33}] = \lceil GJ + Tk_a^2 + EB_1 \left((\theta')^2 + 3\theta'\phi_o' + \tfrac{3}{2} (\phi_o')^2 \right) \rfloor$$

$$+ \Omega^2 \, [I_4] \, \lceil m(k_{m_2}^{\ 2} - k_{m_1}^{\ 2}) \cos 2(\theta + \phi_o) \rfloor \, [I_1]$$

$$[H_{11}] = [H_{22}] = [I_3]\lceil m \rfloor [I_1][I_1]$$

$$[H_{33}] = [I_4]\lceil mk_m^2 \rfloor [I_1]$$

or in condensed notation

$$[G]\{\Phi\} = \omega^2 [H]\{\Phi\} \qquad (11)$$

The submatrices of $[G]$ and $[H]$ are $(n + 1) \times (n + 1)$ square matrices which are functions of blade properties, rotational speed, and the matrix operators $[I_1]$, $[I_2]$, and $[I_3]$. The last element in the submatrices $\{\bar{w}''\}$, $\{\bar{v}''\}$, and $\{\bar{\phi}'\}$ comprising the column matrix $\{\phi\}$ corresponds to the free end of the blade. To satisfy the boundary conditions at the free end of the blade, the $n + 1$, $2(n + 1)$, and $3(n + 1)$ rows and columns of $[G]$ and $[H]$ in equation (11) must be deleted. After performing these deletions, the resulting matrix equations can be cast into the standard eigenvalue form

$$\frac{1}{\omega^2}\{\Phi\} = [D]\{\Phi\} \tag{12}$$

where

$$[D] = [G]^{-1}[H]$$

and is of order 3n x 3n. The general form of $[I_1]$ is given by equation (7) with $[I_2]$ and $[I_3]$ related to $[I_1]$ by

$$[I_2(f)] = [I_4]\lceil f \rfloor - \text{diag}\,[I_4]\{f\}$$

$$[I_3] = [I_4]\lceil x \rfloor - \lceil x \rfloor [I_4]$$

$$[I_4] = \left([D] - \lceil 1 \rfloor\right)[I_1]$$

and

$$[D] = \begin{bmatrix} 0 & 0 & - & - & - & 0 & 1 \\ 0 & - & - & - & - & 0 & 1 \\ | & & & & & | & 1 \\ | & & & & & | & 1 \\ 0 & - & - & - & - & - & 1 \end{bmatrix}$$

The form of the generalized integration operator is dependent upon the numerical procedure chosen to evaluate the integrals. The present analysis employs the integrating matrix method as derived by Hunter.[4] This method expresses the integrand as a polynomial in the form of Newton's forward-difference interpolation formula. In Hunter's development, all functions are in effect represented by polynomials at the boundaries as well as elsewhere on the beam. Since the polynomials approximate the functions very accurately, the integration of these polynomial representations yield extremely small errors. It should be noted that other numerical methods may be used to evaluate the matrix $[I_1]$.

5. NUMERICAL RESULTS

The blade selected for analysis is the WADC S-5 scale model of Reference 5. This blade was chosen since this reference gives a structural description sufficient for numerical solution as well as experimental data for the natural vibration frequencies. The blade is in effect cantilevered at 0.1016 meters from the center of rotation and the tip of the blade is at a radius of 0.6096 meters. In the experimental program, tests were conducted for various pitch angles, defined by the values of θ as measured at $x = 0.75R$ where R is the radius from the center of rotation to the tip of the blade.

In order to compare numerical results with test data, solutions were computed for cases corresponding to the pitch settings and rotational speeds of the experimental investigation. Physical properties of the WADC S-5 blade, as given in Reference 5, are presented in Table 1. Additional sectional properties needed for this analysis were estimated by assuming an elliptical cross section. These estimated physical properties are presented in Table 2. Numerical results were obtained by using 11 stations, which correspond to ten 0.0508 meter intervals, and employing the integrating matrix given by Hunter[4] for a seventh-degree polynomial approximation. The steady-state twist ϕ_o is determined by iteration from equation (5). This value is used to determine the coefficients of equation (12) which is solved using the double shift QR algorithm.[6]

The experimentally and analytically determined free vibration frequencies are given in Figures 2 and 3. Figure 2 illustrates the comparison for the first and second bending frequencies. Figure 3 shows the comparison for the first torsion frequency. Figure 4 illustrates the effect of steady-state twist on the first torsion natural frequency. The dashed curves were obtained by neglecting the underlined terms in equation (6). The per cent error associated with neglecting these terms is shown in Table 3. The influence of steady-state twist is to reduce the torsional frequencies. Figure 4 illustrates that ϕ_o can result in a decreasing torsional frequency with increasing rotational speed.

6. CONCLUDING REMARKS

A numerical method for determining the free vibration characteristics of a rotating blade having high twist and nonuniform spanwise properties is presented. The equations which govern the bending and torsional motion of such a blade are solved using a generalized integration matrix. By using this matrix as an operator on the equations expressed in matrix notation, the differential equations are numerically integrated to eliminate the spatial dependence and reduce to familiar matrix eigenvalue form from which the dynamics of the blade are determined using standard eigenvalue extraction techniques. A comparison of analytical results and experimental data indicates that the method of solution yields very accurate natural frequencies. Steady-state twist was found to have a significant influence on the torsional frequency.

7. REFERENCES

1) Houbolt, John C., and Brooks, George W.: Differential Equations of Motion for Combined Flapwise Bending, Chordwise Bending, and Torsion of Twisted Nonuniform Rotor Blades. NACA Rep. 1346, 1958.

2) White, William F., Jr., and Malatino, Raymond E.: A Numerical Method for Determining the Natural Vibration Characteristics of Rotating Nonuniform Cantilever Blades. NASA TM X-72, 751, 1975.

3) Vakhitov, M. B.: Integrating Matrices as a Means of Numerical Solution of Differential Equations in Structural Mechanics. Izvestiya VUZ. Aviatsionnaya Tekhnika, No. 3, 1966, pp. 50-61.

4) Hunter, William F.: Integrating-Matrix Method for Determining the Natural Vibration Characteristics of Propeller Blades. NASA TN D-6064, 1970.

5) Carpenter, J. E., and Sullivan, E. M.: Structural and Vibrational Characteristics of WADC S-5 Model Propeller Blades. WADC TR 56-298, 1957.

6) Wilkinson, J. H.: The Algebraic Eigenvalue Problem, Clarendon Press (Oxford), 1965.

TABLE 1. Physical properties of propeller blade (Cantilevered at 0.1016 m; station length 0.0508 m).

X/R	m, $N\text{-}sec^2/m^2$	EI_1, $N\text{-}m^2$	EI_2, $N\text{-}m^2$	θ, deg	THICKNESS, m	CHORD, m
1.0	$.495 \times 10^{-3}$	$.024 \times 10^6$	$56. \times 10^6$	-10.0	.1438	6.656
.9	.495	.025	51.4	-7.4	.1412	6.542
.8	.517	.026	47.2	-4.1	.1430	6.369
.7	.528	.027	44.4	0.0	.1480	6.196
.6	.550	.032	43.8	4.8	.1600	6.052
.5	.572	.042	43.8	9.9	.1710	5.864
.4	.616	.057	44.4	14.7	.1970	5.666
.3	.631	.082	45.8	20.0	.2260	5.533
.2	.715	.115	47.9	25.4	.2590	5.331
.1	1.034	.347	63.9	30.9	.3320	5.148
.0	13.200	3.50	250.0	36.0	5.0000	4.899

TABLE 2. Estimated physical properties of propeller blade assuming elliptical cross section.

X/R	GJ, $N\text{-}m^2$	$k_m = k_a$, m	k_{m_1}, m	k_{m_2}, m	B_1, m^6	B_2, m^5
1.0	4.27×10^4	1.66	.0359	1.66	5.76	0.0
.9	3.97	1.63	.0353	1.63	5.19	0.0
.8	4.02	1.59	.0357	1.59	4.60	0.0
.7	4.32	1.55	.0370	1.55	4.14	0.0
.6	5.36	1.51	.0400	1.51	3.97	0.0
.5	6.34	1.47	.0427	1.47	3.63	0.0
.4	9.33	1.42	.0493	1.41	3.52	0.0
.3	13.79	1.38	.0565	1.37	3.59	0.0
.2	19.75	1.33	.0648	1.33	3.41	0.0
.1	40.51	1.29	.0830	1.28	3.68	0.0
0.	2000.00	1.75	1.2500	1.23	60.00	0.0

TABLE 3. Comparison of experimental and analytical torsion frequency.

θ @ .75R DEG	Ω rpm	ω, Hz EXPERIMENTAL	COMPUTED $\Phi_0 = 0$	COMPUTED $\Phi_0 \neq 0$	PERCENT ERROR $\Phi_0 = 0$	$\Phi_0 \neq 0$
-20	1586	201.4	209.7	203.8	4.1	1.2
	2554	198.1	214.8	199.8	8.4	.8
	3587	192.7	222.9	194.4	15.7	.9
	4449	188.2	231.7	190.0	23.1	1.0
	5134	186.8	239.9	187.6	28.4	.4
0	1600	203.9	210.2	206.1	3.1	1.1
	2610	203.9	216.1	206.0	6.0	1.0
	3585	204.5	224.3	206.5	10.0	1.0
	5886	214.1	251.5	215.7	17.5	.7
20	1572	205.8	209.7	207.7	1.9	.9
	2542	207.5	214.8	209.8	3.5	1.1
	4476	216.3	231.0	218.1	6.8	.8
	6016	226.1	248.4	229.8	9.9	1.6
40	1482	205.3	208.6	207.6	1.6	1.1
	2536	207.6	212.5	209.9	2.4	1.1
	5975	223.4	236.7	226.7	5.9	1.5
60	1491	204.6	207.6	206.4	1.5	.9
	2682	204.1	210.0	206.2	2.9	1.0
	4523	204.8	215.9	205.8	5.4	.5
	5945	202.4	221.8	205.6	9.6	1.6

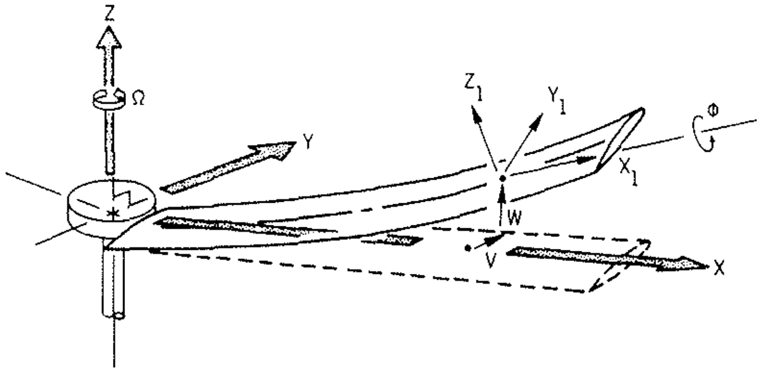

Figure 1.- Blade coordinate systems and deflections.

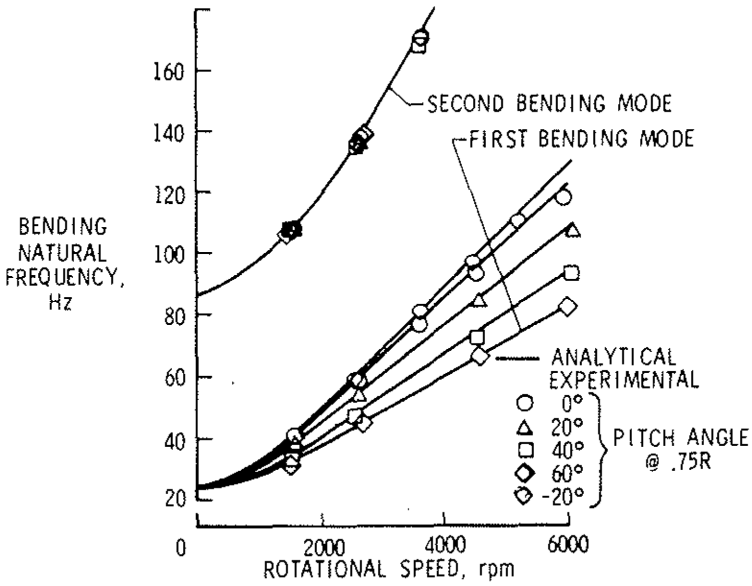

Figure 2.- Variation of bending frequencies with rotational speed.

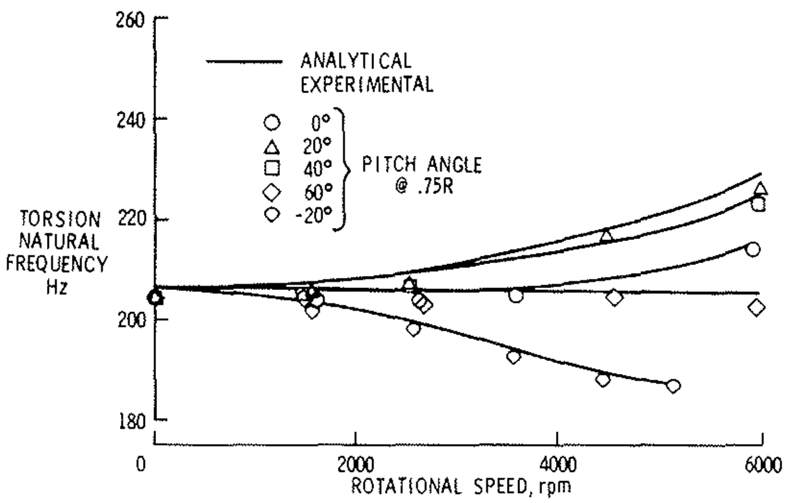

Figure 3.- Variation of torsion frequency with rotational speed.

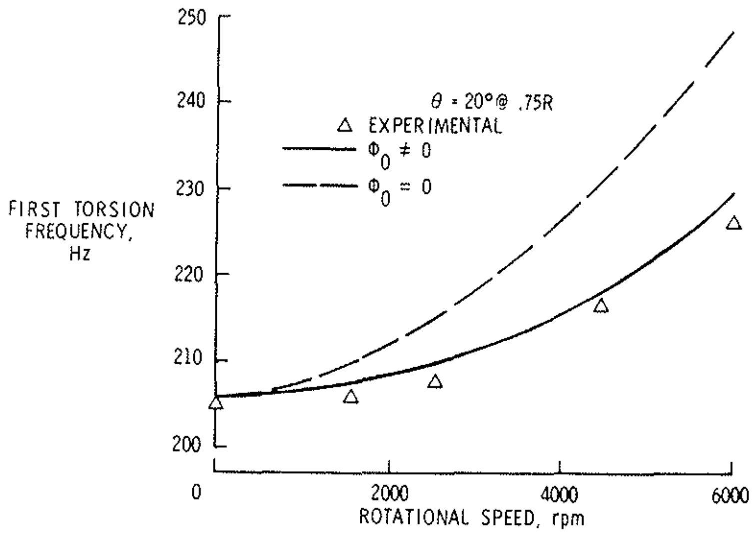

(a) $\theta = 20^{\circ}$ at 0.75R.

Figure 4.- Torsional frequency versus rotational speed.

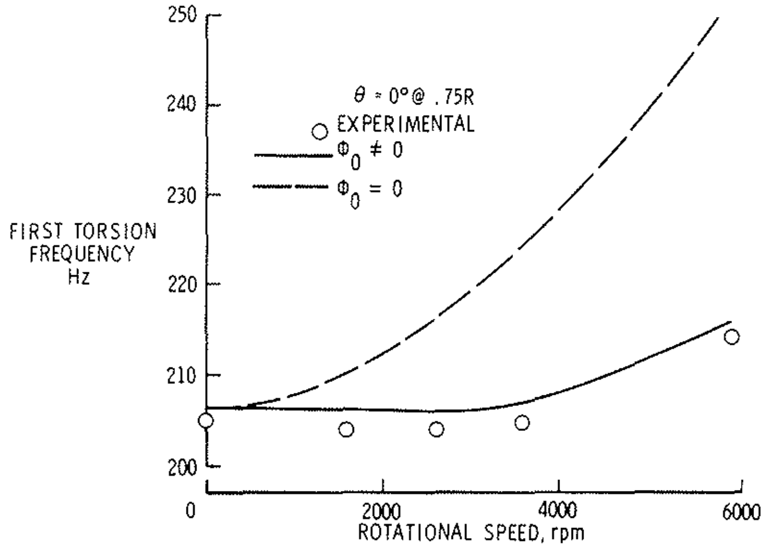

(b) $\theta = 0^{\circ}$ at 0.75R.

Figure 4.- Continued.

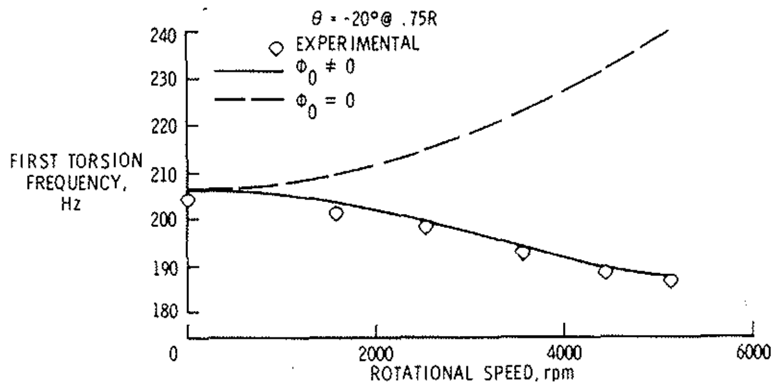

(c) $\theta = -20^{\circ}$ at 0.75R.

Figure 4.- Concluded.